

Numerical and experimental validations of the theoretical basis for a nozzle based Pulse technique for determining building airtightness

Edward Cooper¹, Xiaofeng Zheng^{*2}, Christopher J Wood²

¹ Department of Architecture and Built Environment, Faculty of Science and Engineering, University of Nottingham Ningbo China, 199 Taikang East Road, Ningbo 315100, China

² Buildings, Energy and Environment Research Group, Faculty of Engineering, University of Nottingham, University Park, Nottingham NG7 2RD, UK

*Corresponding author: xiaofeng.zheng@nottingham.ac.uk

Abstract

Motivated by intentions of avoiding large net fluid flow and enabling a more practical airtightness test for large buildings, a low-pressure Pulse pressurisation technique was developed for measuring building airtightness at pressures that are considered more representative of that experienced by buildings under natural conditions. Due to the short and dynamic operation, this technique is able to minimize wind and buoyancy effects during the measurement of building pressure. The investigation, based on the “quasi-steady” temporal inertia model, explores a technique that generates a pressure pulse inside a building by releasing a known amount of air pulse over 1.5 second using a compressed air tank. The volumetric flow rate of the air pulse released from the tank is obtained by measuring the transient pressure in the air tank during a test run. The air leakage through the building envelope is then obtained by accounting for the compressibility of indoor air. Simultaneously, the pressure variation within the envelope of test building is monitored. Therefore, the leakage-pressure relationship of the building envelope can be obtained. The validity of the theoretical model and the assumptions on which the model is based are validated using experimental and numerical investigations.

Keywords

Building airtightness; The Pulse technique; Unsteady approach; Steady pressurisation method; Experimental and numerical validations;

Nomenclature

Symbol

A	Area of opening (m^2)
a, b	Coefficients of quadratic equation for the pressure-flow relationship
B	Constant determined by the shape of the cross-section of the opening.
C	Flow coefficient ($\text{m}^3 \cdot \text{s}^{-1} \cdot \text{Pa}^{-n}$)

d	Diameter of opening (m)
L	Depth of opening (m)
p_i	Building indoor pressure, Pa;
$P(t)$	Transient pressure of air in the air tank
$\dot{P}(t)$	Change rate of building air pressure (Pa/s)
P_0	Initial pressure of air in the compressor
ΔP	Building pressure (Pa)
$\Delta p\{t\}$	Real time building pressure, (Pa)
Q	Air leakage rate (m^3/s)
Q_4	Air permeability at 4 Pa ($\text{m}^3/\text{h}/\text{m}^2$)
Q_{50}	Air permeability at 50 Pa ($\text{m}^3/\text{h}/\text{m}^2$)
ΔQ	Measurement uncertainty of air leakage rate (m^3/h);
$Q_p\{t\}$	Transient volumetric flow rate of tank air, (m^3/s)
$q\{t\}$	Transient building air leakage rate, (m^3/s)
R	Gas constant, equal to $287.058 \text{ J}/\text{kg} \cdot \text{K}$;
T_0	Initial air temperature in the air tank
V	Building volume (m^3)
V'	Volume of air tank (m^3)

Greek letter

μ_i	Viscosity (Pa·s)
ρ_i	Indoor air density, (kg/m^3)
γ	Specific heat of air, 1.4
δQ	Overall error in obtaining the leakage rate, (%)
δQ_B	Bias error, (%)
δQ_P	Error caused by building pressure sensor accuracy, (%)
δQ_M	Model error, (%)

32

33 **1. Introduction**

34 **1.1. Background**

35

36 Defined as the unintentional movement of air through building envelope driven by the pressure
37 difference induced under natural conditions, building infiltration is uncontrolled and impacts
38 upon building energy use and ventilation. Therefore, good understanding of building

39 infiltration is of high importance and typically requires the measurement of building
40 airtightness as a practical and quick alternative to a direct measurement of building infiltration
41 [1], which is disruptive, complex and time consuming.

42 Airtightness is a physical property of a building fabric indicating the envelope integrity and
43 fundamentally determines the level of infiltration. A good level of airtightness in buildings is
44 desirable in most regions where either indoor heating or cooling is required because studies
45 have shown building energy consumption caused by unintended building air leakage can
46 account for 13%-50% and 4%-20% of the overall heating and cooling demand, respectively [2,
47 3, 4, 5, 6, 7]. This represents a significant proportion of global energy usage considering
48 buildings are responsible for up to 40% of that and this figure goes up to 50% in developed
49 countries [8, 9, 10]. However, designers need to be aware that the indoor air quality can be
50 compromised if the building envelope is overly airtight, because indoor contaminants will not
51 be diluted effectively via the infiltration. A purpose-designed ventilation strategy will therefore
52 be required to provide sufficient fresh air for the indoor environment. Another important
53 factor, implicated by airtightness, is the long-term impact made by moisture transportation
54 through the building fabric. The air exchange between indoor and outdoor environments is
55 enhanced by poor building airtightness which then leads to the formation of condensation
56 within the building fabric, consequently deteriorates the fabric and encourages the growth of
57 air pollutants.

58 It has been recognised for decades that airtightness is an important indicator of building
59 integrity and construction quality, which is essential for buildings with good energy efficiency
60 and indoor environment [11, 12]. Over the last few decades, global targets on the achievement
61 of improved indoor environment at low energy cost in the building sector have witnessed the
62 formalisation of minimum requirements on building airtightness in many countries either in
63 building regulations or voluntary standards.

64

65 **1. 2. Conventional Airtightness Measurement**

66

67 In the conventional steady pressurisation test, known as the ‘blower door’, the airtightness
68 measurement is typically done by installing a fan into an existing doorway within the envelope
69 and taking several steady state measurements at multiple elevated pressures (typically 10 to
70 60Pa). Two typical setups (door fan and duct fan) are illustrated by the schematic diagrams in
71 Figure 1. One of the main challenges in such a test is to measure building pressure accurately
72 under natural conditions due to the uncertain and dynamic nature of environmental conditions
73 (particular wind) experienced by buildings. These environmentally induced pressure
74 differentials normally lie in the vicinity of 1-4 Pa [13, 14, 15, 16, 17], which presents a
75 challenge to the accurate measurement of low building pressure as these natural effects can
76 present significant noise. In order to obtain a reliable leakage-pressure correlation, this ‘noise’
77 needs to become a negligible component in the calculation. The random nature of these natural
78 effects mean that such goal is difficult to achieve, so instead steady state measurements are
79 taken at elevated pressure differentials thereby reducing the impact of the low-pressure noise.

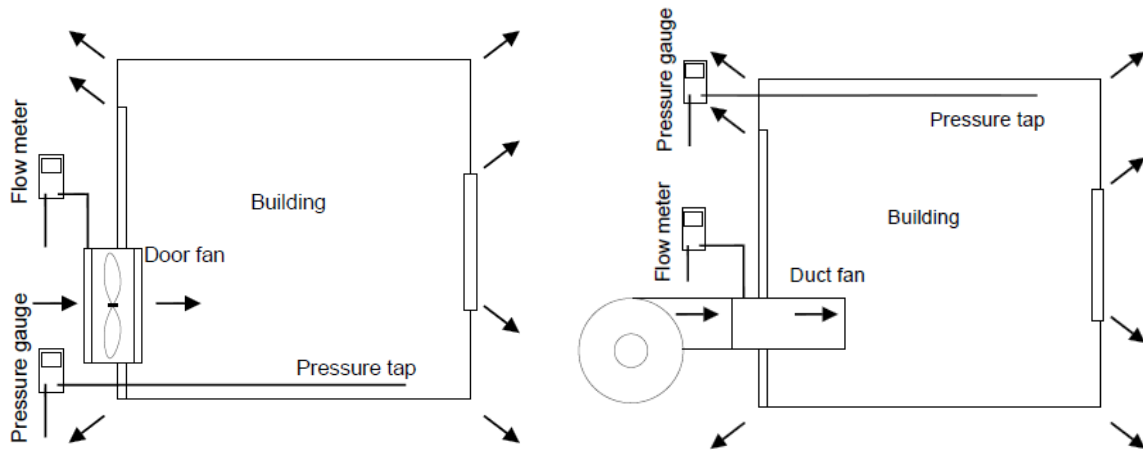


Figure 1 The conventional way of measuring building airtightness -steady pressurisation method (door fan and duct fan: in pressurisation)

81

82 While the ‘blower door’ method has been broadly accepted as the standard means of measuring
 83 building leakage, there have been longstanding uncertainties about its accuracy [18, 19, 20, 21,
 84 22, 23]. Sherman [24] investigated the uncertainties in typical field situations derived from
 85 precision error, bias error and modelling error. Suggestions were made therein to reduce these
 86 uncertainties by taking various measures.

87 The authors believe that large uncertainties are sometimes inevitable [25] in the conventional
 88 steady approach especially when it is used to determine low-pressure leakage, where “direct
 89 measurement of air permeability at infiltration pressures could reduce the uncertainty by a
 90 factor of three or more” [26].

91 Further shortcomings have been discussed in scientific and practical studies [27, 28, 29], and
 92 mainly fall under three aspects: testing practicality, legislation and testing accuracy. The
 93 latter can be expanded on as follows:

- 94 • Coarse interpretation of background pressure during testing [30].
- 95 • Unreliable external pressure reference (especially under windy condition) [31].
- 96 • Uncertainty in extrapolating results down to low pressure.
- 97 • Not testing the whole envelope.
- 98 • Likelihood of opening of additional leakage pathways.
- 99 • Unrealistic high measuring pressure considering hydraulically dissimilar flow at high
 100 and low pressure [13, 14, 32] .

101 Some of these factors contribute to the conventional test method having a margin of error. This
 102 impact on the performance gap has been discussed extensively by the Zero Carbon Hub [29]
 103 and Sherman [33, 34, 35]. Enabling building construction professionals to obtain airtightness
 104 test results more conveniently and efficiently could assist in the pursuit of higher quality
 105 construction. It is also desirable to test the airtightness of a building at lower pressure
 106 differentials, such that the flow through the envelope will mimic that of a building under
 107 ambient pressures. Such factors have provided the research motivation to seek for alternative

108 methods to overcome some of the issues shown in the steady pressurisation method [36].
109 Among which, the Pulse technique was originally developed to overcome the large net fluid
110 flow and uneven pressure distribution associated with testing large buildings [37, 38, 39] by
111 proposing a unsteady method that can be implemented flexibly to determine building
112 airtightness at low pressures. However, the study presented herein is based on tests performed
113 with a single Pulse unit, which is designed to test residential units and small commercial
114 buildings. For large buildings, the underlying principle is the same but multiple units are
115 required to release air pulse simultaneously to provide sufficient flow during testing.

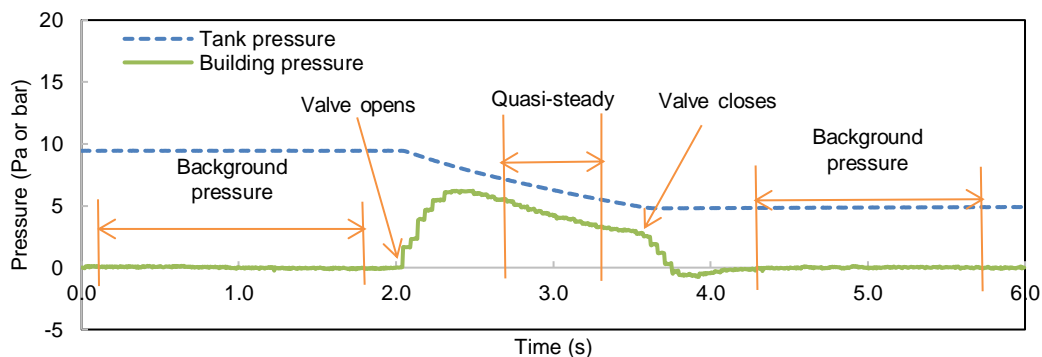
116

117 1. 3. The Innovative Pulse pressurisation technique

118

119 The Pulse technique achieves the measurement by releasing a short air pulse (typically 1.5
120 seconds) into the building from a compressed air system. A subsequent pressure increase in the
121 building is instantly created, which is then followed by a steady pressure drop to deliver a
122 'quasi-steady' flow through the building envelope. During that process, pressure and
123 temperature variations in the building and tank are measured with a sampling rate of 50 Hz to
124 quantify in real time the delivered airflow rate from the tank and stored air in the building due
125 to compressibility to establish the building's leakage-pressure correlation. The background
126 pressure induced by environmental conditions is accounted for in the data treatment and the
127 method used for the adjustment is implemented by removing background pressure trend from
128 direct pressure measurement. More technical details on how that is implemented are described
129 by Cooper et al [32]. Figure 2 shows a typical Pulse measurement, where readings of both tank
130 and building pressures are illustrated comprising pressure variations during the quasi-steady
131 period and background pressure trends before the valve opens and after the valve closes. For
132 the tank pressure readings, only the readings during the quasi-steady period are processed to
133 determine the mass flow rate of released air in real time, whereas for the building pressure, the
134 readings during quasi-steady period are used to account for the compressibility of air and the
135 background pressure readings are used for pressure adjustment to account for the wind and
136 buoyancy effects, i.e. the aforementioned background pressure.

137

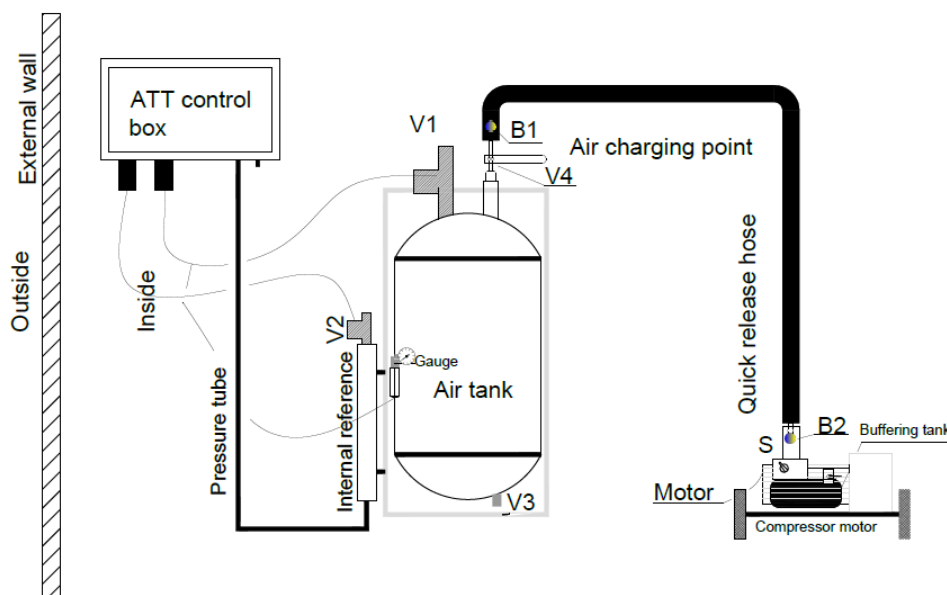


138

139 Figure 2 Pressure measurements of a typical Pulse test (tank pressure measured in bar, building pressure in Pa)
140 [25]

141

142 To demonstrate the system structure of a typical Pulse unit and how the system works, a
 143 schematic diagram is created and shown in Figure 3. It is a standard single-tank unit comprising
 144 an air compressor (oil-free), an air tank for the storage of compressed air and a control panel
 145 used to control the actions of automated valves and acquire readings from pressure and
 146 temperature sensors. This unit is configured to measure the airtightness of small buildings, i.e.
 147 residential unit and small commercial building. Multiple tanks can be linked together to
 148 increase the test capacity to measure large buildings. The maximum working pressure of the
 149 main air tank is set to 10 bar for considerations of system cost, portability and desired unit
 150 capacity. During the Pulse test, ambient air is charged into the air tank by the compressor
 151 through a quick release air hose to a desired pressure level, usually depending on the size and
 152 leakage of the test building. Then the compressed air is discharged into the building over a
 153 short period of time (typically 1.5 seconds) through an electronically controlled solenoid valve
 154 (V1). The pressures and temperatures of the air in the tank and building are respectively
 155 measured by pressure transducers and temperature sensors, mounted within the air tank and
 156 control box. The building integrity is maintained by adopting an internal pressure reference
 157 tank in the measurement of building pressure. This reference tank is an airtight vessel, which
 158 provides a useable pressure reference prior to the measurement by closing the valve (V2)
 159 during the measurement and opening when the test is completed to allow the pressure inside to
 160 equalise with the ambient environment. Therefore, the Pulse measurement is independent of
 161 external pressure condition as it provides a useable pressure reference based on the indoor
 162 pressure so the building pressure response to the added air pulse can be measured. Such feature
 163 allows the Pulse technique to differ itself from the conventional method, which has to rely on
 164 the presence of stable and representative outdoor pressure to achieve an accurate measurement
 165 of pressure changes when the building is subjected to addition or removal of air at a certain
 166 rate.



167

168

Figure 3 System diagram of single-tank Pulse unit [42]

169

1. 4. Aims and objectives

The Pulse technique entails a dynamic approach for measuring building airtightness at low pressures. Due to the transient nature of this testing procedure, the principle and accuracy of the Pulse test is frequently questioned by peer scientists and practitioners in the field.

This paper aims to present a comprehensive introduction on the theoretical background of the technique where the working principle and theoretical model are detailed. The validity of the theoretical model and assumptions on which the model is based is experimentally and numerically validated.

2. Theoretical perspectives

2. 1. Theory and historical development

The initial working concept of the Pulse technique is shown in Figure 4, which illustrates a volume (V) of a single zone with an opening in the envelope. A piston device which is capable of making a volume change of ΔV is installed in the envelope to provide an induced pressure change by introducing a piston movement. The piston moves in the cylinder over time (t) and introduces a piston airflow to the indoor space at a volumetric airflow rate of Q_p , which consequently increases the indoor pressure and simultaneously generates a rate of airflow through the opening (q). Such procedure has evolved to be simpler and more practical at a later stage and can be implemented through releasing a pulse of air via a nozzle directly from a compressed air tank; more details are introduced in the latter part of this section.

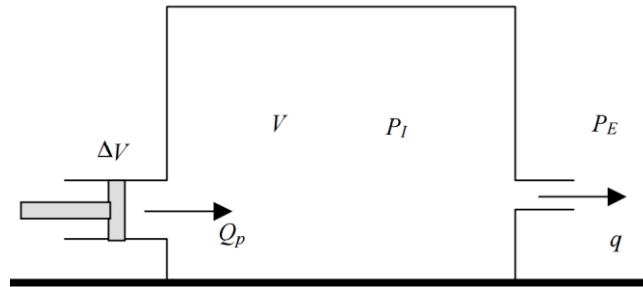


Figure 4 Envelope of a single zone volume with an opening acted on by a piston movement [40]

Following the continuity equation, the airflows through the building envelope during the piston movement can be described by eq.(1):

$$\frac{1}{\rho_i} V \frac{d\rho_i}{dt} = Q_p\{t\} - q\{t\} \quad (1)$$

Where, $Q_p\{t\}$, $q\{t\}$ and ρ_i are the real time volumetric flow rate of air introduced into the envelope by the piston movement, the rate of airflow leaving the envelope through the opening

201 and density of indoor air, respectively. The term on the left of the equation accounts for the
 202 compressibility of the air in the space, which is one of the key factors for achieving good
 203 accuracy in this approach.

204
 205 When isentropic expansion is assumed in this process, the relationship between density ρ_i
 206 and pressure P_i can be obtained as $P_i/\rho_i^\gamma = C$, where C and γ are a constant and specific heat
 207 ratio of air respectively, and $\gamma = 1.4$. Therefore, eq.(1) changes its form to

$$208 \quad q\{t\} = Q_P\{t\} - \frac{V}{\gamma P_i} \frac{dP_i}{dt} \quad (2)$$

209
 210 Based on the same principle, when the piston movement is replaced by a pulse of compressed
 211 air released from an air tank as described in section 1. 3 (Figure 3), the volumetric flow rate of
 212 the air pulse released into the volume by the air tank can be determined by eq.(3):

$$213 \quad Q_P\{t\} = -\frac{V'}{\gamma \rho_i R T_0} \left[\frac{P(t)}{P_0} \right]^{\frac{1-\gamma}{\gamma}} P'(t) \quad (3)$$

214
 215 Where, V' is the volume of air tank (m^3); $P(t)$, P_0 , T_0 and ρ_i are the transient tank air pressure
 216 (Pa), tank air pressure (Pa) and temperature (K) before the release of air pulse and density of
 217 indoor air (kg/m^3), respectively; R and γ are the gas constant ($J/kg \cdot K$) and specific heat ratio
 218 of air; $P'(t)$ is the first time derivative of tank air pressure, (Pa/s).

219 Similar to the leakage measurement using a blower door method, the Pulse technique takes the
 220 measurements of building leakage over a range of pressure. It differs itself from the blower
 221 door method by achieving continuous measurement at low pressures in a dynamic manner.
 222 However, due to the rapid and unsteady approach of introducing pressure change to the indoor
 223 air, this technique faces a challenge during the measurement, i.e. the occurrence of the inertia
 224 effect of unsteady airflow through openings, which adds uncertainty to the measurement and
 225 compromises the accuracy [41]. Such flow due to the inertia effect is addressed as unsteady
 226 flow, which should be minimised in order to obtain accurate measurements. More details on
 227 how the unsteady flow is quantified is given in section 1.2 in [42].

228
 229 The development of the Pulse technique has gone through three stages, a unsteady technique
 230 concept of the piston unit driven by gravity [37], a practical prototype of the piston unit driven
 231 by compressed air[32, 40] and the latest more compact and portable nozzle unit [25, 27, 28, 42,
 232 48]. The historical development of the Pulse technique and its experimental investigations has
 233 been summarised by Zheng et al [43]. Experimental validations have been conducted
 234 throughout the described stages [43]; to prove the concept of the technology, validate various
 235 changes made through the developments, including hardware simplifications and firmware
 236 modifications, and also to investigate the impact of various factors to the measurement such as
 237 environmental conditions, unit location and internal barriers. The experimental studies have
 238 been performed both in sheltered laboratory conditions [49, 42] and outdoor natural conditions

239 [25, 44]. Some of them are introduced herein alongside the numerical investigation to prove
240 the validity of the theoretical model on which the Pulse technique is based.
241

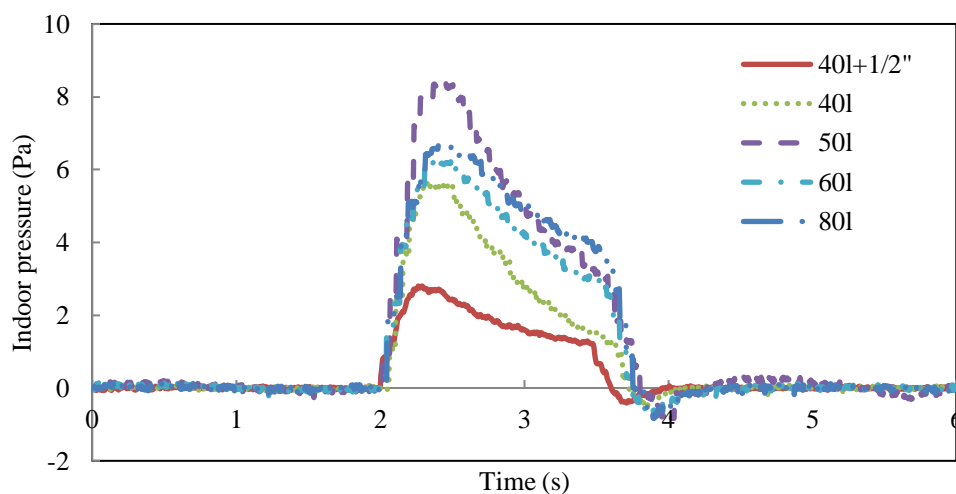
242 2. 2. Impact of tank size and opening length on inertia flow

243
244 The concept of the Pulse technique or a similar approach (AC pressurisation method) has been
245 tried in 1980s [45, 46]. Inertia effect of airflow through the opening has been the major concern
246 for the unsteady method, as it adds uncertainty to the test results [41]. The inertia term is the
247 third one on the right side of eq.(1) given in [42], representing the weight of unsteady flow.
248 When the area of the opening is fixed, it is ruled by the time dependant gradient of building
249 leakage rate $\frac{dq}{dt}$ and the length of opening l_e . The former is determined by the configuration of
250 the unit used for testing and selection of testing period while the latter depends on the physical
251 form of test building.

252 In order to evaluate how the unit configuration and capacity affects the percentage of unsteady
253 flow, tests were carried out using units with various tank sizes, including 40 l, 50 l, 60 l and 80
254 l, all of which used $\frac{3}{4}$ " valve. An additional configuration where the 40 l tank with a smaller
255 valve ($\frac{1}{2}$ "") was used for comparison with the $\frac{3}{4}$ " valve to investigate the impact of valve size
256 on the unsteady flow.

257 Figure 5 shows the pressure pulses produced in a three-bedroom detached house with an
258 internal volume of 343 m^3 by the five different tank and valve combinations. For the 40 l, 60 l
259 and 80 l with the same type of tank, the pulse magnitude extends higher when the tank size
260 increases. But the increase in the magnitude is not significant. It is due to the same starting
261 pressure and outlet size. However, the pressure gradient varies with the tank size, i.e. the greater
262 the tank size, the smaller the pressure gradient is. Noticeably, the magnitude produced by the
263 50 l tank is larger than 60 l and 80 l tank. The tank size and magnitude rule could have been
264 invalidated by the tank of different kind, which perhaps leads to different discharge coefficient.

265



266

267

Figure 5 Pulses produced by different tank and valve combinations

268

269 Results show a negligible amount of unsteady flow was experienced by all the combinations,
270 which suggests reasonable accuracy in the measurement of building leakage is achievable for
271 them all, more details are described by Cooper et al in [25]. By using different tank and valve
272 combinations, the tank pressure drop rate can be affected, which in turn affects the ‘quality’ of
273 the quasi-steady period of a pulse test because it determines how quickly the building pressure
274 drops. This explains why the pressure decay section (from the point where the valve closes)
275 can’t be used for data analysis as it is affected by the inertia effect thereby giving a poor
276 accuracy. Such inertia effect is reflected by the pressure dip in Figure 5. Similar issue is also
277 present when a building is too leaky or too large as in this case there is insufficient flow released
278 from the unit to maintain a steadily decreasing flow, which is a matter of unit capacity and
279 linking with more units can solve this problem. Nevertheless, for standard use the tank and
280 valve combination needs to be configured correctly due to the considerations of its practicality
281 and accuracy.

282

283 The type of opening (building leakage pathway) determines the flow regime. The effective
284 length of opening is discussed in terms of its impact on the inertia effect of airflow through the
285 openings in the building envelope. Taking a pulse test with the 60-litre tank as an example,
286 Figure 6 shows the percentage of unsteady flow given by an opening with various effective
287 lengths. The unsteady flow increases up to 10% from less than 1% when the effective length
288 of opening increases up to 0.5m from 0.05m. Hence, the use of the pulse technique could be
289 limited by the ‘effective length’ of openings in the test building, which is a result of combining
290 a group of openings in the test building, in various length, size and shape. In a way, this
291 relationship can also be interpreted by the electrical analogy, i.e. it is similar to the effective
292 overall electrical resistance when multiple electrical components with different resistances are
293 connected in parallel. Hence, it is worth noting that the effective length of opening discussed
294 herein is different from the dimension of a single opening, for instance, a chimney, but rather
295 an effective hydraulic length of all openings combined [47]. Therefore, the effective overall
296 flow resistance of a network of building leakage pathways is dominated by the ones with small
297 flow resistance, such as short and wide openings.

298

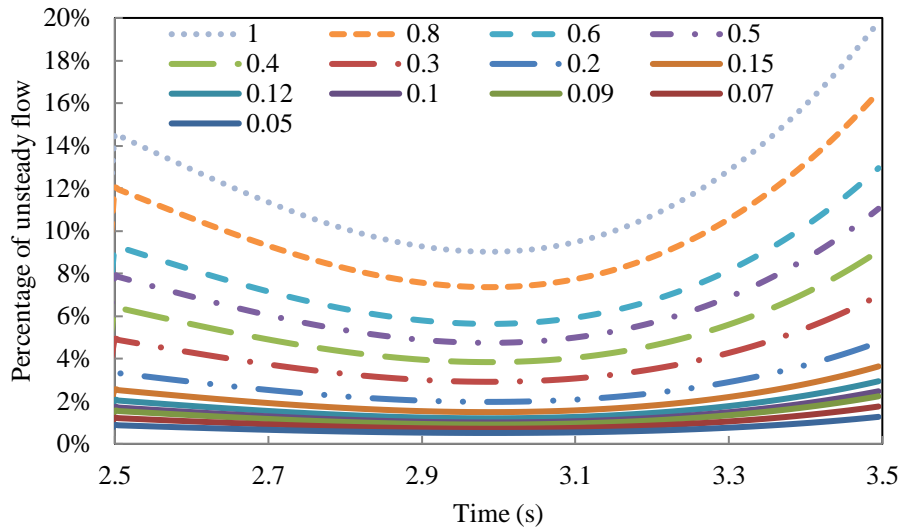


Figure 6 Length of opening (m) vs. percentage of unsteady flow

3. Numerical validation of theoretical model assumptions

The theoretical model described in the previous section determines the building air leakage rate by calculating the transient flow rate of the air pulse released from the compressed air tank and the amount of indoor air that has been stored within the building due to the compressibility of air during the pulse period. Apart from temperature measurements, these calculations largely rely on the measurements of real-time pressures in the air tank and building during testing and therefore the reliability of the calculations is determined by how accurately the pressure measurements represent the actual pressures in the air tank and building. To practically achieve a sufficient accuracy in pressure measurements in both domains using an engineering application, the pressure distributions within them need to be uniform. Therefore, prior to the experimental validation of the accuracy of the Pulse technique for determining the building air leakage rate, these two assumptions on which the theoretical model is based need to be validated first.

3.1. Model and configurations

The assumptions were numerically validated using CFD simulation. ANSYS Fluent was used for the numerical simulation. Energy and momentum equations were discretized using the second-order upwind scheme with transport equations discretized using power law scheme. The SIMPLEC algorithm was used to solve the discretized equations.

For the purpose of validation, the numerical simulation was based on an experimental study where a detached three bedroom house was tested by a Pulse unit with a 80-litre air tank. To save on computation time, the problem was simplified to a two-dimensional axisymmetric

326 domain as shown in Figure 1 in supplemental material 1. The compressed air tank had an orifice
 327 with a diameter of 19.1 mm and a length of 20 mm. The volume of the computational domain
 328 is 290 m³, equal to the volume of the house. The distribution of the leakage pathways in the
 329 envelope is not considered herein but represented by a circular opening with an area of 0.0404
 330 m², which was obtained in an experimental study. A mix of quad and triangular cells were
 331 used to mesh the whole domain with finer mesh applied to the areas inside and adjacent to the
 332 air tank for a more detailed computation. Coupled heat transfer condition was specified at the
 333 walls of the nozzle and air receiver. The building opening was set as pressure outlet with a
 334 constant pressure of 101325 Pa. Initially, the temperature in the whole computational domain
 335 was T₀=288.16 K; the absolute pressure in the compressor air receiver and nozzle was 879200
 336 Pa and the pressure in the remaining area was set at 101325 Pa.

337 The real time building and tank pressures are of interest. Hence, the problem was defined as
 338 transient. Considering the air is compressible, the air used in the simulation was treated as
 339 ideal-gas and the density-based solver was used to provide the density-pressure relationship.
 340 Energy equation was used in conjunction with realizable K-epsilon with scalable wall
 341 functions. Building opening was set as pressure outlet and the gauge pressure is set as 0 Pa (i.e.
 342 absolute pressure 101325 Pa), which means there was insignificant pressure difference between
 343 indoor and outdoor. Patch function was used to apply initial starting pressure to the tank air.
 344 The building pressure was not patched as it was the same with the operating pressure, i.e.
 345 101325 Pa. The size of the time step Δt is determined by eq.(4):

$$346 \quad \Delta t \leq \Delta x / u \quad (4)$$

347 Where, Δx is the smallest cell in the domain, and u is the corresponding velocity in that cell.

349 The smallest cell is located at the orifice, which has a radius of 9.55mm with 9 cells, making
 350 $\Delta x = 1.06$ mm. The velocity at the orifice can be calculated using the flow rate as $u = \frac{Q}{A} =$
 351 $540m/s$, where Q is the volumetric flow rate and A is the geometric area of the orifice. Hence,
 352 $\Delta t \leq 1.06/540 = 1.96 * 10^{-6}$ s. In order to numerically calculate 1.5 second pulse flow, the number
 353 of time steps is determined as $1.5 / 1.96 * 10^{-6} = 764150$, but for the ease of post CFD analysis,
 354 the number of time steps was set as 750000.

355 The silencer, which is attached to the nozzle, helps diffuse the compressed air into the test
 356 building, consists of meshed steel housing and sintered PE. In the numerical simulation, the
 357 configuration of the silencer has been simplified into a porous jump media according to the
 358 flow resistance. Its parameters are listed in Table 1.

360 Table 1 Settings of porous jump media

Parameters	Face permeability (m ²)	Porous medium thickness (m)	Pressure-Jump Coefficient (1/m)
Value	1e+11	0.012	1900000

361

362 **3. 2. Results and discussions**

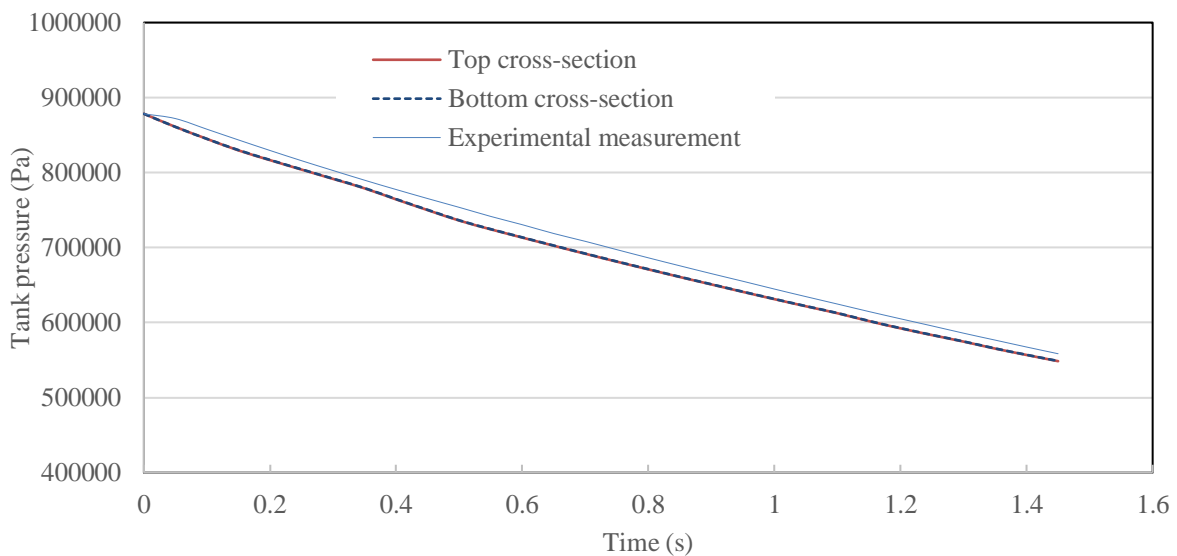
363 **3.2.1. Uniformity of air pressure in the compressed air tank**

364

365 The derivation of Eq.(3) is based on the assumption that the pressure in the tank is uniform
366 during the pulse period. Therefore, the uniformity of air pressure over the time of testing needs
367 to be verified.

368 To provide an example, Figure 2 in supplementary material 1 shows the contour of pressure
369 distribution in and around the bottom half of the tank at 0.0s and 0.5s. It can be noted that the
370 pressure contour in the nozzle is different from that in the tank. That is caused by the airflow
371 occurred during air releasing process but does not affect the pressure distribution in the tank.
372 The pressure contour in the tank indicates the pressure variation across the air tank is minimal.
373 To further check the uniformity of the tank air pressure, the real time variation of area-averaged
374 pressure at top and bottom cross-sections were tracked as illustrated in Figure 2 (a) in
375 supplementary material 1. Figure 7 shows the pressure difference between the two cross-
376 sections is unremarkable. Therefore, the pressure distribution in the tank can be considered
377 highly uniform and only one pressure transducer should suffice for the measurement. However,
378 the location of the sensor needs to avoid the impact of air movement for optimal accuracy.
379 Hence, the mounting position should be distanced from the tank orifice/nozzle.

380



381 Figure 7 Comparison of tank pressure variations during the pulse period in experimental measurement and
382 numerical simulation with the area-averaged pressures at top and bottom cross-sections
383

384

385 Figure 7 shows the transient tank pressures during the 1.5-second pulse period obtained in the
386 experimental measurement and numerical simulation. The pressures given by the numerical
387 simulation are smaller than those given by the experimental measurements, but within 2.4%.
388 This might be caused by the difference in temperature condition between numerical simulation
389 and experimental setup during the pulse period due to different heat transfer occurred through
390 the tank and nozzle walls. Nevertheless, a good agreement between them was demonstrated.

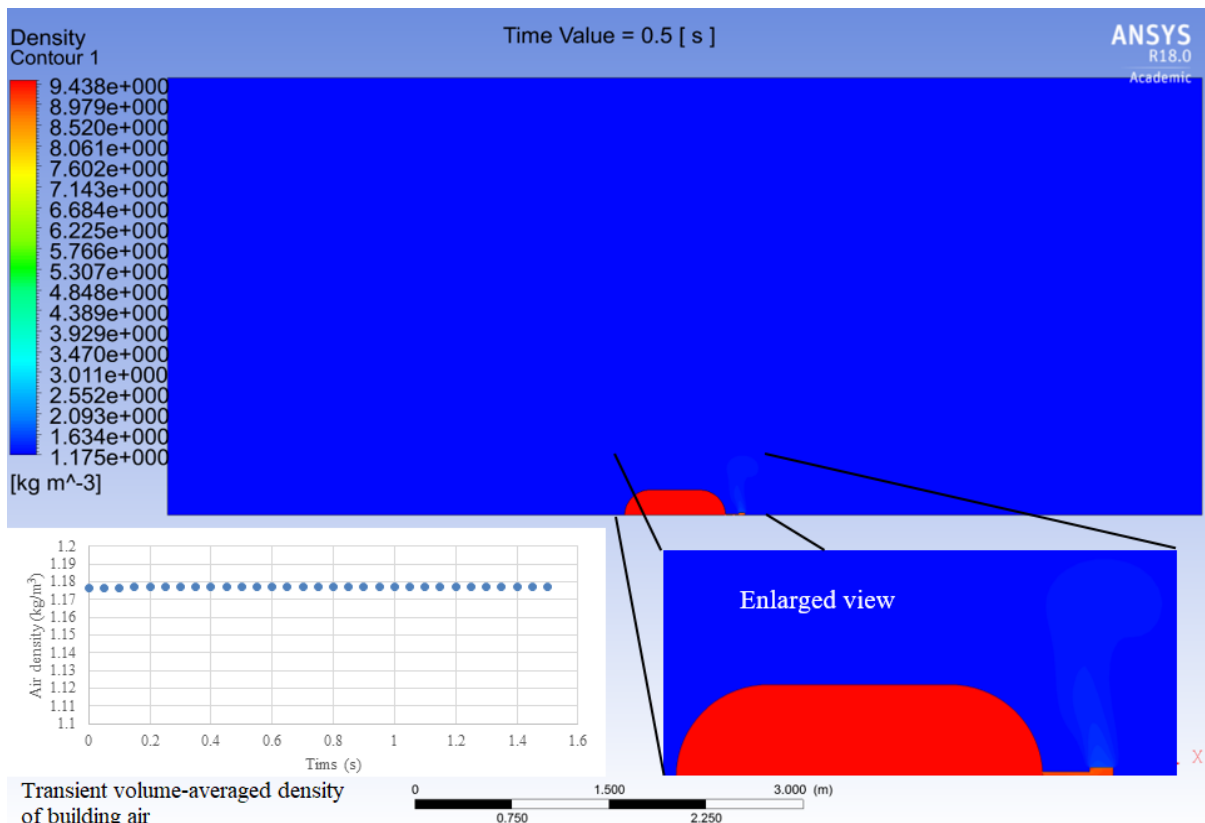
391

392 **3.2.2. Uniformity and invariability of air density in the building envelope**

393

394 To confirm eq.(3) is valid for calculating $Q_p\{t\}$, the density of air within the building envelope
395 must be uniform and invariable during the whole pulse period. Figure 8 shows the density
396 distribution of air around the nozzle when $t=0.5s$. It can be noted that there is a relatively
397 obvious gradient of air density in the region near the outlet of the compressor nozzle. However,
398 the area represents a very small part of the whole domain and the effect on the air density in
399 the test space is highly likely to be insignificant.

400 To check the uniformity of density during the pulse period, the volume-averaged density $\bar{\rho}\{t\}$
401 in the simulated building envelope is used. To confirm the invariability of the air density during
402 the pulse period, the variation of volume-averaged density with time within the simulated
403 building envelope is illustrated by a graph embedded at bottom left corner of Figure 8. It can
404 be noted that, during the pulse period, the change of $\bar{\rho}$ is very small, with a change of 0.06%
405 during the period of $0 \leq t \leq 1.5$. Therefore, the impact to overall density distribution caused
406 by the uneven density distribution near the nozzle outlet can be considered negligible, and good
407 uniformity is present in the test space during a pulse test. This result was agreed by an initial
408 experimental study on the pressure distribution of a five-bedroom house [48].



409

410

Figure 8 Density distribution (kg/m^3) around the nozzle when $t=0.5s$

411

4. Experimental validations of the Pulse test

Through development, the Pulse technique has utilised two different methods to deliver a known volume of air into the test building. The initial version (piston unit) relied upon a compressed air mechanism to drive a large piston to move over a set distance in a known length of time to introduce pressure change to the building. The nozzle unit achieves such pressure change by discharging a pulse of compressed air into the building directly from a compressed air tank via a nozzle. Both methods rely upon the same fundamental principle defined above. But the piston unit relies on the velocity of the piston's movement, whereas the nozzle unit determines the mass flow rate more directly from the pressure variation in the compressor tank. This necessitates the measurement of tank pressure and temperature in order to calculate the flow rate of the air pulse released from the tank. Therefore, the experimental validations of current nozzle-based Pulse technique consist of the one against the original piston unit and the other against the conventional steady pressurisation method.

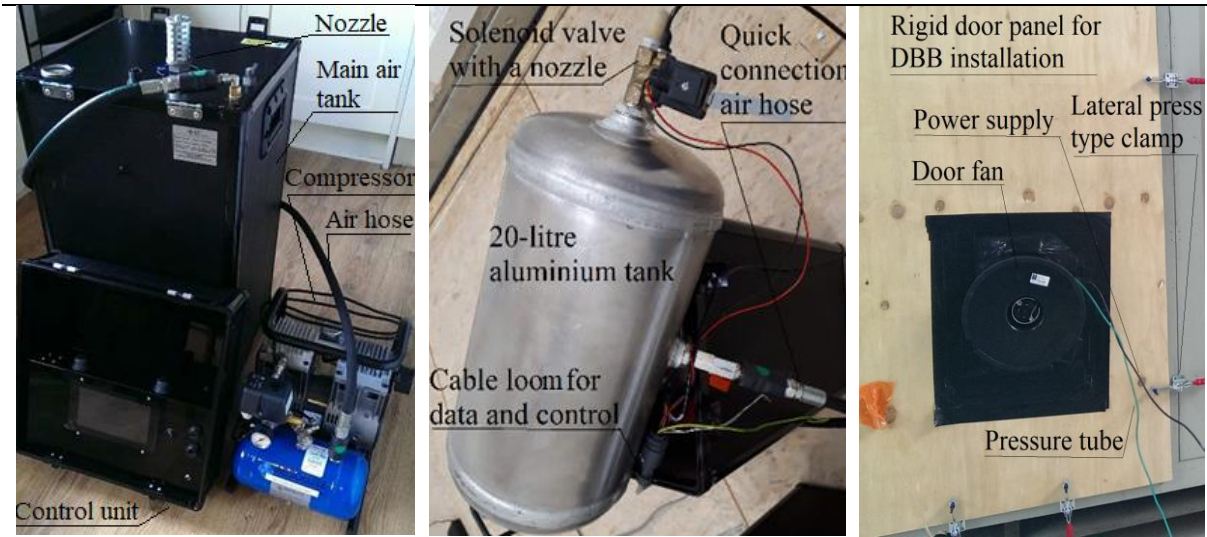
4.1. Experimental setup and testing arrangement

The building used for the comparison between the nozzle unit and the piston unit has a volume of 136.1 m³ and an envelope area of 185.8 m² with a cube shape. A sheltered chamber, which is 16 m³ in volume and 40 m² in envelope area, was used for testing to compare the nozzle unit with the blower door technique.

In the first experimental validation, the nozzle unit at stage 3 was compared with the piston unit at stage 2 [43]. In the second one, Duct Blaster B (DBB), a low range Minneapolis blower door, was utilised for comparison with the stage 5 Pulse unit. The DBB comprises a small variable-speed fan, a pressure-flow gauge, an adjustable door frame and a flexible canvas panel. It is designed to take more accurate readings in the low range of fan flow than larger models. Therefore, it was utilised in the comparison tests with the PULSE-40/20 units, as listed in Table 2.

Table 2 Pulse and blower door units used for comparison

PULSE-40 (cased)	PULSE-20 (without casing)	Energy Conservatory Duct Blaster B
------------------	---------------------------	------------------------------------

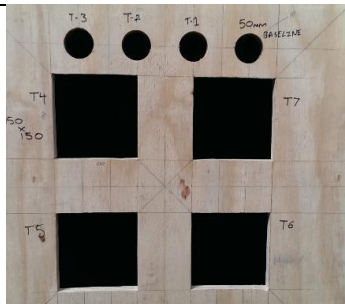


442
 443 The Pulse units incorporated a lightweight aluminium tank (39.8 litre and 20.1 litre) and a
 444 double piston compressor. The outlet utilises a ½ inch (PULSE-40) and ¼ inch (PULSE-20)
 445 (BSP) automated fast responding valve to discharge compressed air into the chamber from the
 446 air tank over 1.5 seconds. The corresponding pressure and temperature signals are taken and
 447 processed by the control unit.

448
 449 Table 3 Setup of the DBB and test plates in the chamber



Setup of the DBB in the chamber



Testing plate A with a number of well-defined openings



Testing plate B with three circular holes (two extended by pipes)

451 As listed in Table 3, two test plates were used for testing, herein named as test plate A and B.
452 The test plate A has four square (150mm×150mm) and four circular (diameter: 50mm) short
453 and sharp-edged openings in the middle of the plate, similar to holes that might be found in
454 construction material layers or in window frames. Test plate B has three circular openings with
455 tubular pipes connected to the top two openings. Plate B seeks to represent those openings
456 found in service penetrations such as ventilation ducts or cable casing running through the wall.
457 More details about the various testing scenarios are given in [49]. During testing, these plates
458 were installed with screws on the opposite side of the fenestration where the DBB was
459 mounted. Wing screws were utilised to fix the plate onto the external surface of the chamber
460 wall.

461
462 Eight different testing scenarios were achieved by sealing up various combinations of openings
463 in the two plates. Table 1 in supplemental material 2 shows the details of how the eight testing
464 scenarios were prepared using sealing tapes. Each testing scenario was named according to the
465 testing order, from scenario T0 to scenario T7. For instance, the blower door tests were
466 performed first in scenario T0. After the scenario T0 was completed, a piece of sealing tape
467 was removed to introduce one more opening to the scenario T1, and this testing procedure was
468 repeated until the scenario T7 was completed. The same testing process was repeated for the
469 Pulse unit after the blower door testing was completed. One pressurisation test was run in each
470 scenario while the Pulse test was repeated three or four times in each scenario, except scenarios
471 T6 and T7, where the test could only be performed twice due to the time constraint at the end
472 of testing. This testing arrangement allowed both testing methods to be subject to various
473 leakage characteristics and levels.

474

475 **4. 2. Results and discussions**

476 **4.2.1. Comparison with the piston unit**

477

478 Figure 9 shows the pressure pulses of five repeated tests. The curves are adjusted to account
479 for any variation of Δp caused by environmental conditions but particularly wind during the
480 pulse period to obtain the building pressure change induced by the release of the air pulse [32].
481 Such process is done by fitting a curve to the background pressure trend given by building
482 pressure before and after the pulse, and deducting the curve from the raw measurement. In
483 Figure 9 (left) the wind effect is noticeable as indicated by the fluctuations before and after the
484 pressure pulses, and the quasi-steady period occurs between 0.4 and 1.4 s. The calculated
485 transient mass flow rate for one of the tests is shown in Figure 9 (right).

486

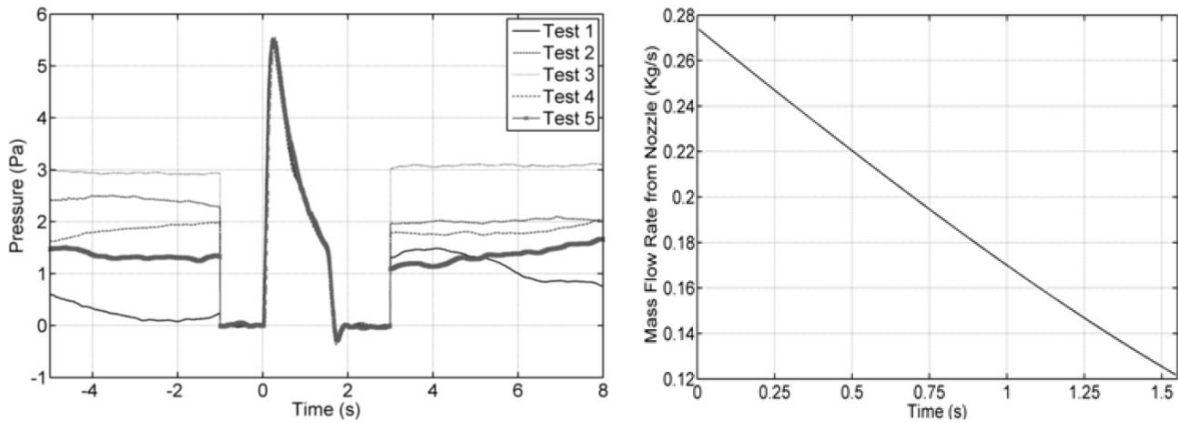


Figure 9 Pressure pulses (left) and transient mass flow rate of the air released from nozzle (right) of five repeated Pulse test

487

488 The good repeatability of the technique can be seen in the plotted $\Delta p(t)_q(t)$ correlation curve
 489 in Figure 10, where the average air leakage rate at 4 Pa was $0.17598 \text{ m}^3/\text{s}$. Further tests were
 490 done to assess the sensitivity of the technique by sealing and unsealing the openings around
 491 the test room door. The technique measured an average difference of $0.01626 \text{ m}^3/\text{s}$, suggesting
 492 the technique is sufficiently sensitive to small changes in leakage.

493 The piston unit (stage 2 in [43]) was tested in the same test room under the same conditions
 494 and the results are illustrated by Figure 11. A good agreement was observed indicating that the
 495 nozzle-based Pulse unit provided consistence results with the piston unit. Interestingly, it is
 496 noticeable that under the same pressure differences slightly lower values of leakage were
 497 consistently given by the piston tests. This discrepancy is attributable to an unavoidable leak
 498 of air from the narrow gap between the piston and cylinder wall during the piston test [43].
 499 Therefore, slightly underestimated leakage $Q_P\{t\}$ could be measured in the piston test because
 500 $Q_P\{t\}$ is obtained indirectly from measuring the displacement of the piston with regard to time
 501 using a cable extension transducer. Nevertheless, the results suggested that the nozzle approach
 502 is a valid means of introducing transient pressure change to the test building.

503

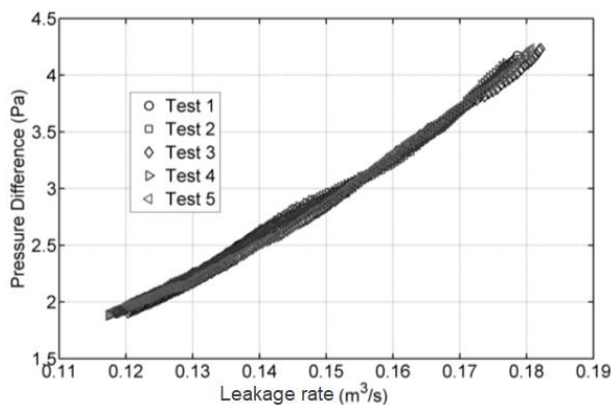


Figure 10 Nozzle test results

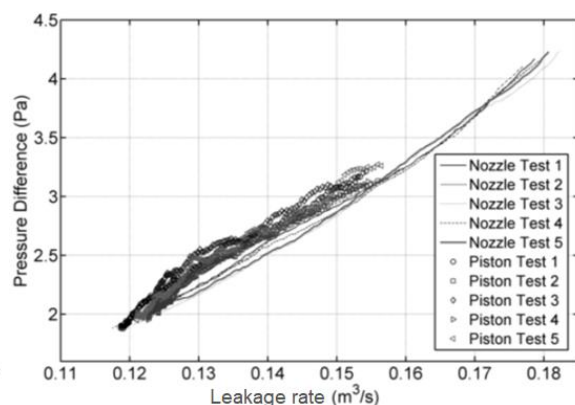


Figure 11 Comparison of nozzle and piston results

504

4.2.2. Comparison with a low range blower door in a sheltered environment

Table 2 in supplementary material 2 lists the leakage-pressure graphs of both tests taken in the chamber in eight scenarios. Crossover in data in most of the scenarios were achieved to provide direct comparison. For instance, in scenario T0 (Figure 12), the lowest point in the overlapped pressure range was at 10 Pa where the difference in test result between the both tests was 8.8% and the highest was at 18 Pa with 4.8% difference. The percentage difference of the test results in all testing scenarios given by both testing methods is summarised in Table 4.

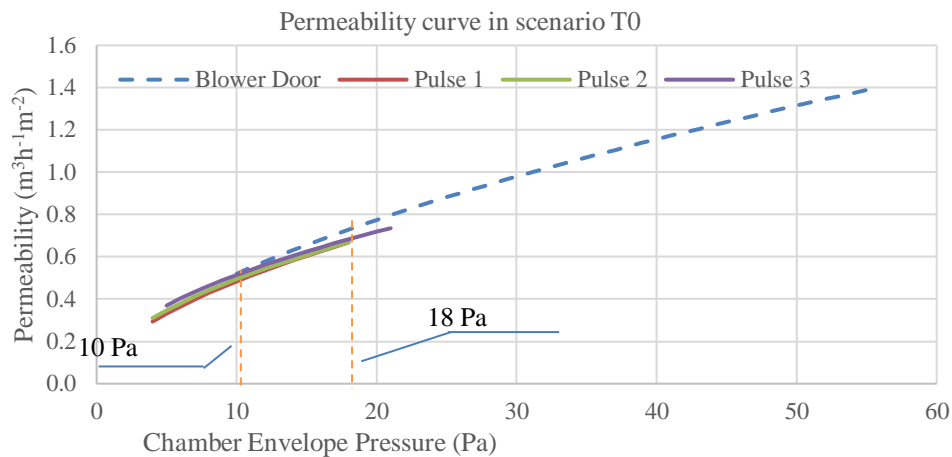


Figure 12 Testing results of scenario T0 [49]

Table 4 Summary of test results given by the blower door and Pulse tests in all scenarios

Scenario	Range of crossover (Pa)	Minimum (%)	Maximum (%)	Average (%)
T0	10-18	4.1%	7.8%	6.4%
T1	5-23	2.5%	7.8%	4.9%
T2	6-16	0.8%	4.1%	1.6%
T3	7-20	0%	2.2%	0.6%
T4	N/A	N/A	N/A	N/A
T5	9-13	6.0%	12.8%	9.6%
T6	16	7.4%	7.4%	7.4%
T7	14-20	3.8%	6.4%	5.5%

Note: N/A means no pressure overlap was achieved.

The results show the difference between both testing methods varies from scenario to scenario with the average difference ranging from 0.6% to 9.6%. Scenario T3 gave the best agreement followed by the scenario T2, both of which showed an average percentage difference less than 2%. The largest difference was seen in the scenario T5 where four circular openings and two square openings were present in the test plate. The openings were lying closely in the centre of the test plate and hence large net fluid flow was generated through the test plate likely creating a ‘pressure sink’ near openings, i.e. non-uniform pressure distribution in the vicinity of openings. This might consequently lead to errors in the pressure measurement, especially so in a small test space and therefore produce larger percentage difference between the two. The average difference in overlap between the blower door and Pulse data is 6.0%. Although this testing does not yield a consistent offset that may be accounted for as all testing comes with an inherent level of measurement uncertainty, with BS EN ISO 9972:2015 [50] citing an overall

531 uncertainty of lower than $\pm 10\%$ in calm conditions for the blower door fan and the
532 manufacturer citing $\pm 5\%$ uncertainty for Pulse measurements [25]. In this context, the level of
533 agreement is generally encouraging, especially for test scenario T2, T3 and T7. A similar
534 finding was reported by Zheng et al [42] in another comparison study where both testing
535 methods were utilised to measure the leakage of a sheltered house-sized chamber, which was
536 set up with various leakage scenarios and levels. Therefore, the Pulse technique is able to
537 provide measurements that are in close agreement with the blower door method.

538

539 **4. 3. Error analysis**

540

541 The measurement uncertainty of the experimental validation is evaluated to assess the
542 confidence level of the results. Considering the purpose of the comparison with the piston unit
543 essentially serves the development of the nozzle-based Pulse unit and their working principles
544 are similar, the error analysis herein is therefore focused on the experimental study where the
545 latter is validated against the blower door unit.

546 Theoretically, the overall error in obtaining the leakage rate at a given pressure level comprises
547 those errors caused by instrumentation accuracy (bias), background pressure induced by
548 environmental conditions (precision) and modelling (model) [24]. In order to illustrate the
549 sources of error in obtaining the leakage rate using the Pulse and blower door methods, an error
550 source diagram is created, as shown in Figure 13. Due to some similarity between both testing
551 methods, five error sources are shared by them. They are mainly related to the measurement of
552 building parameters such as dimensions, pressure and temperature as well as model
553 specification. Other error sources are from the measurement of the airflow delivered by each
554 method to pressurise the building. For the Pulse method, it is the combination of measurements
555 of volume, air pressure and temperature of the tank that is used to determine the delivered
556 airflow from the air tank corrected by the room air temperature, while for the blower door
557 method, the delivered airflow is determined by the fan flow but corrected by indoor and outdoor
558 air temperature. The overall error in obtaining the leakage rate can be described by eq.(5):

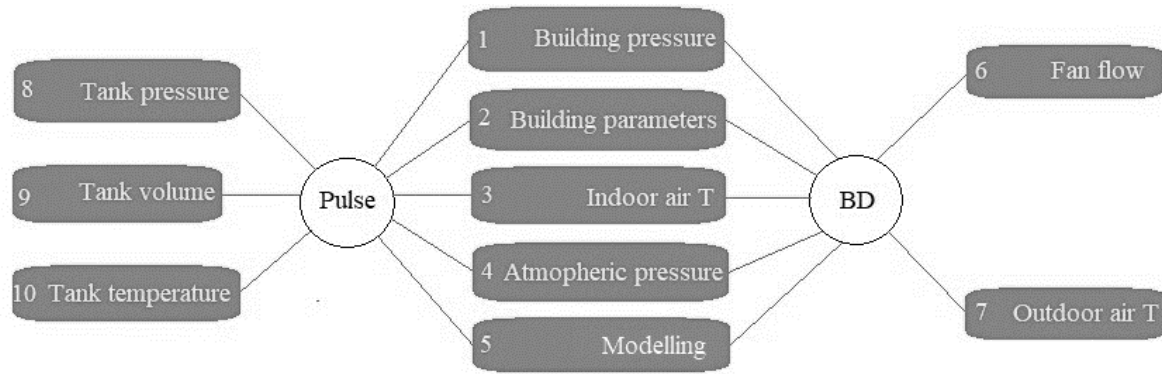
559

$$\delta Q = \sqrt{\delta Q_B^2 + \delta Q_P^2 + \delta Q_M^2} \quad (5)$$

560

561 Where, δQ , δQ_B , δQ_P and δQ_M are the overall error in obtaining the leakage rate, bias error
562 and error of leakage rate at the quoted pressure level caused by the building pressure sensor
563 accuracy and model error, respectively.

564



565

566 Figure 13 Source of error in the Pulse and blower door test (BD) (Note: No.1 Building pressure represents the
 567 building pressure response to the added or removed air in the airtightness test; for blower door, it is the
 568 difference between indoor and outdoor pressure; in the Pulse test, it is the difference between indoor pressure
 569 and reference tank pressure)

570

571 Table 5 summarises the measurement uncertainty of each error source and the three main error
 572 types with the responsible error sources. For the model error δQ_M , it is defined as the deviation
 573 between the mathematical model predictions and the measurements. It should be noted that the
 574 model error herein is mainly determined by model specification but also varies with the
 575 measurement of chamber pressure. Hence, the model error appraised in this study also contains
 576 the impact of environmental condition to the chamber pressure measurement and an average
 577 error across the overlapped pressure range is taken for analysis.

578

579

Table 5 Summary of error source for both testing methods

ID	Error source	Accuracy (%)	
		Blower door	Pulse
1	Building pressure (Pa)	±0.9%	±0.25%
2	Building parameter (m ³ or m ²)	±10% [50]	
3	Indoor air temperature (°C)	±0.2	±0.08
4	Atmospheric pressure (hPa)	±3	N/A
5	Modelling	0.45%-1.79%	0.60%-3.90%
6	Fan flow (m ³ /h)	±3.0%	N/A
7	Outdoor air temperature (°C)	±0.2	
8	Tank air pressure (Pa)	N/A	±0.2%
9	Tank volume (litre)		±0.4
10	Tank air temperature (°C)		±0.08

Error type	Bias (δQ_B)	Precision (δQ_P)	Model (δQ_M)
Note	Instrumentation accuracy	Weather condition	Model specification
Error source ID	Blower door: 1, 3, 4, 6, 7 Pulse: 1, 2, 3, 4, 8, 9,10	Blower door: 1 Pulse: 1,	Blower door: 1, 5 Pulse: 1, 5

580

581 For the Pulse measurement, the analysis of instrumentation caused error (bias) has been
 582 described in details in [42]. Due to the fact the test was carried out in a sheltered environment,
 583 the impact of the environment condition on the measurement of chamber pressure is minimised
 584 but still reflected in the reading of chamber pressure and therefore it is included in the analysis.
 585 The theoretical support of the Pulse technique is fundamentally based on the quadratic
 586 equation, which is used to understand the Pulse performance and determine a reliable

587 configuration that is able to accurately measure the building leakage over a range of pressure.
 588 However, the power law equation, as widely used and accepted mathematical representation of
 589 the leakage-pressure relationship, is used in both tests to describe the building's leakage-
 590 pressure relationship for simplicity and user friendliness. Therefore, the error of calculating the
 591 leakage rate using the power law equation at the quoted pressure level due to the measurement
 592 accuracy of chamber pressure (δQ_p) can be described by eq.(6).

593

$$\delta Q_p = \frac{(1 \pm \delta P)^n - 1}{1} \quad (6)$$

594

595 Where, P and δP are the chamber pressure and accuracy of chamber pressure sensor,
 596 respectively.

597

598 Using eq.(5), the overall error in obtaining the chamber leakage rate in the sheltered condition
 599 using the both methods in all the test scenarios are calculated and the results are listed in second
 600 and third row of Table 6. The results show that in the validation tests the blower door has
 601 delivered measurements with overall error below 3.5% in all eight scenarios, with most
 602 scenarios in close vicinity of 3%. For the Pulse tests, most of the scenarios have obtained an
 603 overall error below 3.5%, except for the scenario T5, which is slightly higher at 4.4%.

604

605

Table 6 Overall error of both testing methods and combined error in comparison

Scenario	T0	T1	T2	T3	T4	T5	T6	T7
Blower door	±3.14%	±3.23%	±3.10%	±3.13%	±3.05%	±3.07%	±3.19%	±3.53%
Pulse	±3.01%	±2.31%	±2.18%	±2.53%	±3.62%	±4.39%	±2.41%	±2.30%
Comparison	±6.15%	±5.54%	±5.28%	±5.65%	±6.68%	±7.47%	±5.60%	±5.83%

606

607 When both testing methods are used to measure the chamber leakage under the same scenario
 608 for comparison, the resulted maximum difference between the measurements given by both
 609 testing methods against the measured leakage rate can be calculated, as shown in the bottom
 610 row of Table 6. Compared to the average relative percentage difference between the results
 611 given by both testing methods listed in Table 4, the overall errors obtained in all the test
 612 scenarios fall outside the error range by 0.25%-2.13%. Considering the factors (such as
 613 equipment setup, chamber preparation etc.) leading to difference in the chamber leakage
 614 between both tests might not be fully eliminated during testing, such error is considered
 615 acceptable for the purpose of validation.

616

617 The error analysis presented here only assesses the confidence level of the comparison between
 618 the measurements given by both testing methods as part of the experimental validation. In
 619 practice, the measurement uncertainty at the referenced pressure especially at a low level is
 620 often of concern due to the greater wind impact and should be discussed. However, for the
 621 Pulse tests in this study, the measurement uncertainty at 4 Pa falls within the reported values
 622 and therefore is not singled out in the analysis because it doesn't add much value to the
 623 validation purpose and the wind impact was minimised in the tests due to the sheltered
 condition.

5. Conclusions

The Pulse technique for determining the adventitious leakage of buildings at low pressures has been developed to overcome some of the issues experienced by the conventional steady pressurisation method. As an unsteady approach, the challenge for the Pulse technique lies in minimising the inertia effect of unsteady flow through building openings, which is common in the unsteady flow conditions. The presence of unsteady flow adds uncertainty to the measurement and leads to compromised accuracy when it represents a significant proportion in the overall flow. The key reasons why the Pulse technique works are due to the consideration of compressibility of the air and the use of quasi-steady temporal inertia model, which is the underlying principle of the Pulse technique because it is able to quantify the unsteady flow by isolating the unsteady term in the momentum equation. Such that the correct unit configurations can be identified to deliver accurate and repeatable measurements. The theoretical model for determining the mass flow rate of the air pulse released from the nozzle is based on assumptions that the pressure distribution in the air tank and test building is uniform. Numerical investigations and experimental validations showed that the assumptions are true and that the results of both tests in a sheltered environment agreed with each other well. The experimental validations against the steady pressurisation method in various leakage scenarios under a sheltered environment where the impact of outdoor weather condition was reduced have achieved a good agreement between the tests by both testing methods. The error analysis to the experimental validations has proved that the results are reliable. Therefore, the Pulse technique can be considered a feasible and accurate low pressure approach for measuring building airtightness.

ACKNOWLEDGEMENTS

The authors gratefully acknowledge funding received from: the European Union's Horizon 2020 research and innovation programme under grant agreement No 637221. ['Built2Spec': www.built2spec-project.eu/]; the European Union's Seventh Programme for research, technological development and demonstration under grant agreement No 314283. ['HERB': www.euroretrofit.com/]; and the Innovate UK programme for 'Scaling Up Retrofit' under project No: 101609. ['PULSE': www.pulseairtest.com/]. The experimental data used for verifications in this study was obtained in collaboration with Build Test Solutions Ltd in a project supported by Department for Business, Energy and Industrial Strategy Energy Entrepreneurs Fund Scheme, Phase 5 (EEF5029).

Finally, the authors particularly wish to acknowledge the late Dr David Etheridge, whose inspirational research laid the foundation for the work reported here.

REFERENCE

-
- [1] A.V. Pasos, X.F. Zheng, L. Smith, C.J. Wood
Estimation of the infiltration rate of UK homes with the divide-by-20 rule and its comparison with site measurements
Building and Environment, 185 (2020), November 2020, 107275.
- [2] S.J. Emmerich, et al
Impact of infiltration on heating and cooling loads in U.S. office buildings
Department of Energy, Office of Building Technologies. Agreement No. DE-AI01-01EE27615
- [3] S.J. Emmerich, A.K. Persily
Energy impacts of infiltration and ventilation in U.S. office buildings using multizone airflow simulation
IAQ and Energy 98, P.191-203
- [4] J. Jokisalo, J. Krunitski, M. Korpi, T. Kalamees, J. Vinaha
Building Leakage, infiltration, and energy performance analyses for Finnish detached houses
Building and Environment 44 (2009) 377-387
- [5] G Raman, K Chelliah, M. Prakash, R.T.Muehleisen
Detection and quantification of building air infiltration using remote acoustic methods
In: Inter.Noise, Melbourne Australia, 16-19 November 2014
- [6] Keast D.N., Pei H.S
The use of sound to locate infiltration openings in buildings
Proceedings *ASHRAE/DOE Conference* "Thermal performance of the exterior envelopes of buildings", Florida, December 3-5. 1979
- [7] H.Ross
Air Infiltration," Lecture at Public Meeting
DoE, Division of Building and Community Systems, Architectural and Engineering Systems Branch, 21 September 1978
- [8] UNEP
Buildings and Climate Change, Summary for Decision-Makers
Sustainable Buildings & Climate Initiative. Available from:
<http://www.unep.org/sbci/pdfs/SBCI-BCCSummary.pdf>
- [9] L. Lombard, J. Ortiz, C. Pout
A review on buildings energy consumption information
Energy and Buildings 40 (2008) 394-398
- [10] International Energy Agency
Transition to Sustainable Buildings-Strategies and Opportunities to 2050
Available from:
<http://www.iea.org/Textbase/npsum/building2013SUM.pdf>
- [11] D. Etheridge

A perspective on fifty years of natural ventilation research
Building and Environment. Volume 91, September 2015, Pages 51-60

[12] AIVC
Air infiltration instrumentation and measuring techniques
In: 1st AIVC Conference, Windsor, Berkshire, UK, 6-8 October; 1980

[13] D. Etheridge
A perspective on fifty years of natural ventilation research
Building and Environment. Volume 91, September 2015, Pages 51-60

[14] M.H. Sherman, R.Chan
Building Airtightness: Research and Practice
Lawrence Berkeley National Laboratory Report (2004), Report No. LBNL-53356

[15] M. Sandberg, M. Mattsson, H. Wigo, A. Hayati, L. Claesson, E. Linden, M. A. Khan
Viewpoints on wind and air infiltration phenomena at buildings illustrated by field and model studies
Building and Environment (2015), 92, pp. 504-517

[16] Modera M (1991)
Cited in ASHRAE fundamentals
Atlanta: American Society of Heating, Refrigerating and Air-Conditioning Engineers, 2009.

[17] A.V. Pasos, X.F. Zheng, M. Gillott, C. Wood
Experimental study on the pressure differential at which building air leakage should be measured
In: 18th International Conference on Sustainable Energy Technologies, Kuala Lumpur, Malaysia, 20-22 August 2019

[18] Persily, A.K. 1983
Repeatability and accuracy of pressurisation testing
Thermal Performance of the Exterior Envelopes of Building II, pp. 380-390. Atlanta: American Society of Heating, Refrigerating, and Air-Conditioning Engineers, Inc.

[19] Persily, A.K. 1984
Air flow calibration of building pressurization devices
National Bureau of Standards, Report NBSIR 84-2849

[20] Persily, A.K., R.A. Grot. 1985
Accuracy in pressurization data analysis
ASHRAE Transactions, Vol. 91, Part 2B, pp. 105-119

[21] Dickinson, J.B., H.E. Feustel. 1986a
Influence of wind on the accuracy of blower door measurement: A numerical study
Unpublished report.

[22] Gadsby, K.J., and D.T. Harrje. 1985
Fan pressurization of building: Standards, calibration, and field experience

ASHRAE Transactions, Vol. 91, Part 2B, pp. 95-104

[23] Murphy W.E., Colliver D.G., Piercy L.R.

Repeatability and reproducibility of fan pressurization devices in measuring building air leakage

IN-91-12-1 (RP-594)

[24] Sherman, M.

Uncertainties in fan pressurisation measurements

Airflow Performance Conference 10/93 LBL-32115

[25] E. Cooper, X.F. Zheng, C. Wood, et al

Field trialling of a Pulse airtightness tester in a range of UK homes

International Journal of Ventilation. <http://dx.doi.org/10.1080/14733315.2016.1252155>

[26] Cooper EW, Etheridge DW (2007)

Determining the adventitious leakage of buildings at low pressure. Part 1: uncertainties.

Building Serv. Eng. Res. Technol. 28, 1 (2007) pp. 71-80

[27] E. Cooper, X.F. Zheng, M. Gillot, S. Riffat, Y.Q. Zu.

A nozzle pulse pressurisation technique for measurement of building leakage at low pressure

In: 35th AIVC Conference “Ventilation and airtightness in transforming the building stock to high performance”, Poznan, Poland, 24-25 September 2014, page 236-243

[28] E. Cooper, X.F. Zheng, C. Wood, et al.

Field trialling of a new airtightness tester in a range of UK homes

In: 36th AIVC conference “Effective ventilation in high performance buildings”, Madrid, Spain, 23-24 September 2015

[29] Zero Carbon Hub

Closing the gap between design and as-built performance: End of term report

July 2014. Available from:

http://www.zerocarbonhub.org/sites/default/files/resources/reports/Design_vs_As_Built_Performance_Gap_End_of_Term_Report_0.pdf

[30] Sherman M.H., Grimsrud, Sonderegger R.C.

The low pressure leakage function of a building

LBL-9162, EEB-Env-79-10.

[31] Modera M.P., Wilson D.J.

The Effects of Wind on Residential Building Leakage Measurements

Air Change Rate and Airtightness in Buildings, ASTM STP 1067, Sherman M.H., Ed., American Society for Testing and Materials, Philadelphia, 1990, pp. 132-144

[32] Cooper EW, Etheridge DW

Determining the adventitious leakage of buildings at low pressure. Part 2: pulse technique

Building Serv. Eng. Res. (2007) Technol; 28: 81-96

[33] M.H. Sherman, N.E. Matson, 2002

Air Tightness of New U.S. Houses: A Preliminary Report

Lawrence Berkeley National Laboratory, LBNL 48671. Lawrence Berkeley National Laboratory, Berkeley, CA

[34] M.H. Sherman, D. Dickerhoff, 1994

Air-Tightness of U.S. Dwellings

In Proceedings, 15th AIVC Conference: The Role of Ventilation, Vol. 1, Coventry, Great Britain: Air Infiltration and Ventilation Centre, pp. 225-234. (LBNL-35700)

[35] M. H. Sherman

Infiltration in ASHRAE's residential ventilation standards

Lawrence Berkeley National Laboratory, LBNL-1220E. Lawrence Berkeley National Laboratory, Berkeley, CA.

[36] Zheng X.F., Cooper E.W., Gillott M., Wood C.J.

A practical review of alternatives to the steady pressurisation method for determining building airtightness

Renewable and Sustainable Energy Reviews (2020), , vol.132, 110049

<https://doi.org/10.1016/j.rser.2020.110049>

[37] Carey PS, Etheridge DW

Leakage measurements using unsteady techniques with particular reference to large buildings

Building Serv. Eng. Res. Technol. 2001; 22: 69-82

[38] Lee D.S., Jeong J.W., Jo J.H.

Experimental study on airtightness test methods in large buildings: proposal of averaging pressure difference method

Building and Environment, Volume 122, September 2017, pp.61-71

[39] Straube J.

Airtightness testing in large buildings

Building Science Digest 040

[40] Cooper EW, Etheridge DW

Measurement of building leakage by unsteady pressurisation

AIVC Conference, Prague, 2004

[41] Sharples S, Closs S, Chilengwe, 2005

Airtightness testing of very large buildings: a case study

Building Serv. Eng. Res. Technol. 26,2 (2005) pp. 167-172.

[42] Zheng X.F., Cooper E.W., Mazzon J., Wallis I., Wood, C.J.

Experimental insights into the airtightness measurement of a house-sized chamber in a sheltered environment using blower door and pulse methods

Building and Environment 2019, Vol.162, <https://doi.org/10.1016/j.buildenv.2019.106269>.

[43] Zheng X. F., Cooper E., Zu Y. Q., Gillott M., Tetlow D., Riffat S., Wood C. J. 2019b.
Experimental Studies of a Pulse Pressurisation Technique for Measuring Building Airtightness

Future Cities and Environment, 5(1), 10

[44] Zheng X.F., Mazzon J., Wallis I., Wood, C.J.

Airtightness measurement of an outdoor chamber using the Pulse and blower door methods under various wind and leakage scenarios

Building and Environment 2020, <https://doi.org/10.1016/j.buildenv.2020.106950>

[45] M. Sherman, M. Modera

Low-frequency measurement of leakage in enclosures

LBL, Applied Science Division, University of California, March 1986

[46] Card W.H., Sallman A., Graham R.W., Drucker E.E.

Infrasonic measurement of building air leakage-a progress report

Proceedings ASTM, ASHRAE, NBS, DOE Symposium on Air infiltration measurements Washington D.C. March 13, 1978.

[47] Zheng X.F., Wood C.J.

On the power law and quadratic forms for representing the leakage-pressure relationship- Case studies of sheltered chambers

Energy and Buildings, Volume 226, 1 November 2020, 110380

[48] Hsu Y.S., Zheng X.F., Cooper E.W., Gillott M., Lee S.K., Wood C.J.

Evaluation of indoor pressure distributions in a detached house using the Pulse airtightness measurement technique

in: 40th AIVC conference, Ghent, Belgium, 15-16 October 2019.

[49] Zheng X. F., Smith L., Moring A., Wood C. J.

Refined assessment and comparison of airtightness measurement of indoor chambers using the blower door and Pulse methods

In: 40th AIVC conference, Ghent, Belgium, 15-16 October 2019

[50] BS EN ISO 9972

Thermal performance of buildings-Determination of air permeability of buildings-Fan pressurisation method

BSI Standards Publication (2015)